

ZDZISŁAW ZATORSKI \*

## DIAGNOSTICS OF BALLISTIC RESISTANCE OF MULTI – LAYERED SHIELDS

In the presented work, the author describes a new diagnostic method of ballistic resistance of multi – layered shields. The proper ballistic energy absorbed by the shield is introduced in the form  $V_{BL[R]}^2$  according to Recht's and Ipson's method, and  $V_{BL[Z]}^2$  according to author's method. The kinetic energy of the bullet  $m_p \cdot V_p^2/2$  and the momentum of force  $I$  are transferred to the shield and the dynamometer of ballistic pendulum. They are used to determine the proper energy  $V_{BL[Z]}^2$  and ballistic thickness  $h_{BL}$  of the shield. The procedure can be widened onto the absorption of the energy by individual layers of the shield, where:  $A_{an,bn}^{Hn}$  – the effect of  $n$  – interlayer on proper energy absorbed by the shield. The effectiveness of the used methods is expressed by average effectiveness coefficient  $\beta_s$  of proper energy absorbed by the shield  $V_{BL}^2$  as well as by average mass coefficients  $\alpha_s^2$ . The ballistic shields can be composed of different grades of metal layers and interlayer areas with well-chosen ballistic proprieties.

The maximization of interlayer effectiveness  $N_{n[R]}$  and  $N_{n[Z]}$  as well as relative mass effectiveness  $M_{s[R]}$  and  $M_{s[Z]}$  leads to optimum conditions of selection of multi – layered shields structures.

### NOMENCLATURE

$A_{an,bn}^{Hn}$	– effect of $n$ – interlayer on proper energy absorbed by the shield, $m^2 s^{-2}$ ,
$E_{abs}$	– ballistic energy absorbed by the shield and the bullet, $(m_{BL} \cdot V_{BL}^2/2)$ , $kg m^2 s^{-2}$ ,
$E_p$	– kinetic energy of the bullet, $(m_p \cdot V_p^2/2)$ , $kg m^2 s^{-2}$ ,
$h_{BL}$	– ballistic thickness, m,
$I$	– impulse of force transmitted to the dynamometer of ballistic pendulum, Ns,

\* Faculty of Mechanical and Electrical Engineering, Naval University of Gdynia, J. Śmidowicza 69, 81-103 Gdynia, Poland; E-mail: z.zatorski@amw.gdynia.pl

$m_{BL}$	– ballistic mass, kg,
$m_p$	– initial mass of the bullet, kg,
$m_{rp}$	– residual mass of the bullet, kg,
$m_{rt}$	– residual mass of the shield, kg,
$N_{n[R]}, N_{n[Z]}$	– interlayer effectiveness,
$M_{s[R]}, M_{s[Z]}$	– relative mass effectiveness,
$V_{BL}$	– ballistic velocity, $\text{ms}^{-1}$ ,
$V_p$	– impact velocity of the bullet, $\text{ms}^{-1}$ ,
$V_r$	– residual velocity of the bullet, $\text{ms}^{-1}$ ,
$V_{BL}^2$	– energy absorbed by the shield $E_{abs}$ per unit mass ( $2E_{abs}/m_p$ ), $\text{m}^2 \text{s}^{-2}$ ,
$V_{BL[R]}^2$	– proper energy absorbed by the shield according to Recht's and Ipson's method, $\text{m}^2 \text{s}^{-2}$ ,
$V_{BL[Z]}^2$	– proper energy absorbed by the shield according to author's method, $\text{m}^2 \text{s}^{-2}$ ,
$\alpha_s^2$	– average mass coefficient,
$\beta_s$	– average effectiveness coefficient of the energy absorbed by the shield.

## 1. Introduction

The improvement of resistance of ballistic shields to penetration was possible through introduction of hardened layers since the end of XIX century [4]. Multi – layered shields consist generally of a hard layer coated on a plastic layer, together absorbing the kinetic energy of the bullet. The ballistic shields should comply with the following requirements in order to assure:

- the protection against specific bullets and parameters of firing;
- the integrality and functionality of the shield and the protected construction under firing;
- the minimum areal density of the shield.

In the result of investigations it has been found that basic requirement for steel armour is its high hardness. However, there exists a nonlinear dependence between the hardness and ballistic velocity  $V_{BL}$ . In the range of lower hardness of sheets, ballistic velocity increases with the shield's hardness, as penetration of the sheet follows as the result of plastic flow of the material. In the range of average hardness, ballistic velocity becomes smaller in the consequence of appearance of adiabatic shear bands [15]. Ballistic shields in the form of dual hardness clad plates (600/440) HB made it possible to reduce ballistic thickness  $h_{BL}$  to 8 mm and to raise mass effectiveness  $M$  to 1.78 against 7.62 mm AP bullets [9], [13]. The effect of the steel plates

thickness occurs for the impact velocity  $V_p$  below  $1000 \text{ ms}^{-1}$  [20]. Generally, the expansion of plastic deformations area in radial direction across successive inclusion of consecutive layers is determined when taking into account cutting and friction on interfaces. It is connected with the increase of ballistic velocity of the shield against simulated bullets [3]. Due to the above-mentioned facts, the thickness of shield  $h_{BL}$  is equal to the depth of bullet penetration  $p$  in a very thick plate. Hitherto, many experimental works were published to assess ballistic resistance of homogeneous and multi – layered shields. The absorption of the energy by multi – layered shields changes with the impact velocity [8], [11], [12]. Positive effect of enlarged aerial spaces was observed also for multi – layered steel armour type MARS 190. Then, the shield type 3 x 10S/50A/50S was introduced instead of perforated plate 80 mm thick, which gave the penetration depth of 45mm [16]. The presented characteristics can be recommended for the design of multi – layered shields.

## 2. Momentum and energy conservation laws

The bullet that has the mass  $m_p$  and the impact velocity  $V_p$  evokes ballistic erosion of the shield and the bullet, and causes that their residual masses  $m_{rt}$  and  $m_{rp}$  escape with residual velocity  $V_r$  on the line of fire. The author introduces the following equations of momentum and energy conservation laws

$$m_p \cdot V_p = (m_{rp} + m_{rt}) \cdot V_r + I, \quad \text{kgms}^{-1} \quad (1)$$

$$\frac{m_p \cdot V_p^2}{2} = \frac{m_{BL} \cdot V_{BL}^2}{2} + \frac{m_r \cdot V_r^2}{2} + \frac{I_2}{2M_e}, \quad \text{kg m}^2\text{s}^{-2} \quad (2)$$

where:

$m_p, m_{rp}, m_{rt}$  – initial and residual mass of the bullet and residual mass of the shield;

$V_{BL}, V_p, V_r$  – ballistic velocity of the shield, the impact velocity and residual velocity of the bullet;

$I$  – the impulse of force transmitted to the dynamometer of ballistic pendulum;

$M_e$  – equivalent mass of ballistic pendulum.

The ballistic mass  $m_{BL}$  is determined by

$$m_{BL} = m_p - \frac{I^2}{M_e \cdot V_p^2}, \quad \text{kg} \quad (3)$$

when  $V_{BL} = V_p$  and  $V_r = 0$ .

In accordance with Recht's and Ipson's method [14], [5] one can determine the relationship

$$V_{BL}^2 = V_p^2 - \frac{(m_{rp} + m_{rt})^2 V_r^2}{m_p^2}, \quad \text{m}^2\text{s}^{-2} \quad (4)$$

Armor – piercing (AP) bullets which perforate ductile plates usually drive very little plate material from plates. Hence, for AP bullets,  $m_r = m_{rp} + m_{rt} = m_p$  and the following equation fits the AP data very well [1], [2], [4], [5]

$$V_{BL[R]}^2 = V_p^2 - V_r^2, \quad \text{m}^2\text{s}^{-2} \quad (5)$$

### 3. Design of ballistic multi-layered shields

In accordance with the results of investigations [1], [2], [4], [8], the dependences (4, 5) can be used in the first approximation as the energy absorbed by the plate during perforation of multi - layered shields. The dependence of the energy absorbed per unit mass  $V_{BL}^2$  ( $V_{BL[R]}^2$ ,  $V_{BL[Z]}^2$ ) versus ballistic thickness of the plate  $h_{BL}$  under normal impact can be described as

$$V_{BL}^2 = b_1 + b_2 \cdot h_{BL} + b_3 \cdot h_{BL}^2, \quad \text{m}^2\text{s}^{-2} \quad (6)$$

where:  $b_1$ ,  $b_2$ ,  $b_3$  – experimentally determined constants.

The proper energy  $V_{BL}^2$  absorbed by metal layers of the shield with interlayer areas can be expressed by

$$V_{BL}^2 = X_{h_1, H_1}^0 + A_{a_1, b_1}^{H_1} + X_{h_2, H_2}^{b_1} + A_{a_2, b_2}^{H_2} + Y_{h_3, H_3}^{b_2} + \dots + A_{a_n, b_n}^{H_n} + X_{h_n, H_n}^{b_{n-1}}, \quad \text{m}^2\text{s}^{-2} \quad (7)$$

where:

$X_{h_1, H_1}^0$ ,  $X_{h_n, H_n}^{b_{n-1}}$  – proper energy absorbed by metal layer of the first grade;

$Y_{h_3, H_3}^{b_2}$  – proper energy absorbed by metal layer of the second grade;

$A_{a_n, b_n}^{H_n}$  – the effect of  $n$  – interlayer on proper energy absorbed by the shield;

$h_n$ ,  $H_n$  – the thickness of  $n$  – metal layer and total thickness of  $n$  – metal layers;

$a_n$ ,  $b_n$  – the thickness of  $n$  – interlayer and total thickness of  $n$  – interlayers.

Then, the structure selection of the shield with taking into account different grades of metal layers and interlayer areas is possible. The solution is obtained for multi layered shields with different air gaps [19] according to experimental data [1]. The relationship (6) for constructional steel plates (S1, S2) that have the yield strength 230 MPa and 315 MPa [1] is expressed by

$$V_{BL1}^2 = 14496 + 12042.6h_{BL} + 2277.74h_{BL}^2, \quad \text{m}^2\text{s}^{-2} \quad (8)$$

$$V_{BL2}^2 = 35351 - 6584.09h_{BL} + 4393.63h_{BL}^2, \quad \text{m}^2\text{s}^{-2} \quad (9)$$

The ballistic thicknesses  $h_{BL} = 14.7$  mm and  $h_{BL} = 12.9$  mm are estimated from the above equations at ballistic velocity  $V_{BL} = V_p = 826.2 \text{ ms}^{-1}$ . In accordance with equations (7, 8), proper energy absorbed by homogeneous steel layers of the shield with air gaps is expressed by

$$X_{4,4}^0 + A_{0,0}^4 + X_{4,8}^0 = 487^2, \quad \text{m}^2\text{s}^{-2} \quad (10)$$

when  $X_{4,4}^0 = 314.8^2$ ,  $A_{0,0}^4 = -109.5^2$ ,  $X_{4,8}^0 = 387.4^2$ ,  $\text{m}^2\text{s}^{-2}$ .

The proper energy absorbed by heterogeneous steel layers with air gaps is expressed by

$$X_{6,6}^0 + A_{0,0}^6 + Y_{8,14}^0 = 784^2, \quad \text{m}^2\text{s}^{-2} \quad (11)$$

when  $X_{6,6}^0 = 410.72^2$ ,  $Y_{8,14}^0 = 727.48^2$ , and  $A_{0,0}^6 = -288.1^2$ ,  $\text{m}^2\text{s}^{-2}$ .

Negative values of  $A_{0,0}^6$  and  $A_{0,0}^4$  show the negative effect of the plate division on thinner layers with air gaps of the shield. The perforation of the shield is the basis for the above-mentioned equations (10, 11). The impact processes which are terminated inside of the shield are described by inequalities. The solution requires estimation of effects of air gaps, and this estimation must be performed on basis of other tests. For example

$$X_{4,4}^0 + A_{8,8}^4 + Y_{8,12}^8 + A_{8,16}^{12} + X_{4,16}^{16} = V_{BL}^2 \geq V_p^2, \quad \text{m}^2\text{s}^{-2} \quad (12)$$

the solution to the inequality is received from results of tests [1], where:  $V_{BL} = V_p = 826.2 \text{ ms}^{-1}$ :  $X_{4,4}^0 = 314.8^2$ ,  $A_{8,8}^4 = -111.8^2$ ,  $Y_{8,12}^8 = 728^2$ ,  $A_{8,16}^{12} = -90.2^2$ ,  $X_{4,16}^{16} = 272.6^2$ ,  $\text{m}^2\text{s}^{-2}$ .

In this case, the penetration of the last layer attains about 3.1 mm depth. The procedure makes it possible to estimate the real ballistic thickness of the shield. The resistance to penetration of multi-layered shields with air, glass and sand interlayers is presented in the next sections.

#### 4. Experimental verification of ballistic effectiveness of constructional shields

##### 4.1. Verification methods of ballistic resistance of constructional shields

For the purpose of further analysis, the proper energy absorbed by the shield  $V_{BL[Z]}^2$  is introduced, when  $m_p = m_r = m_{BL}$

$$V_{BL[Z]}^2 = \frac{2 \cdot I}{m_p} \cdot \left( V_p - \frac{I}{2m_p} \right), \quad \text{m}^2\text{s}^{-2} \quad (13)$$

The impulse of force is transferred to the dynamometer of ballistic pendulum

$$I = \int_0^{T_m} F(t) \cdot dt, \quad \text{Ns} \quad (14)$$

where:

$F(t)$  – the impact force registered on the dynamometer of ballistic pendulum,

$T_m$  – the time at maximum impact force  $F_{max}$ .

In the first approximation, the impact force is presented as

$$F(t) = F_{max} \cdot \sin\left(\frac{\pi \cdot t}{2 \cdot T_m}\right), \quad \text{N} \quad (15)$$

Then, the impulse of force  $I$  is expressed by

$$I = \frac{2 \cdot F_{max} \cdot T_m}{\pi}, \quad \text{Ns} \quad (16)$$

One defines the mass coefficient  $\alpha^2$

$$\alpha^2 = \frac{V_p^2 - V_{BL[Z]}^2}{V_r^2} \quad (17)$$

and the average mass coefficient

$$\alpha_s^2 = \frac{1}{n} \cdot \sum_{k=1}^n \alpha_k^2 \quad (18)$$

The effectiveness coefficient  $\beta_s$  of proper energy  $V_{BL}^2$  is defined as

$$\beta_s = \frac{V_{BL[R]s}^2 - V_{BL[Z]s}^2}{V_{BL[Z]s}^2} \quad (19)$$

The average proper energies  $V_{BL}^2$  are defined as

$$V_{BL[R]s}^2 = \frac{1}{n} \cdot \sum_{k=1}^n V_{BL[R]k}^2, \quad \text{m}^2\text{s}^{-2} \quad (20)$$

and

$$V_{BL[Z]s}^2 = \frac{1}{n} \cdot \sum_{k=1}^n V_{BL[Z]k}^2, \quad \text{m}^2\text{s}^{-2} \quad (21)$$

The experimental verification of the above relationships performed on the basis of tests, which were performed on a unified test stand to investigate ballistic resistance of materials [5], [10]. The test stand is developed, implemented and patented at the Naval University of Gdynia [6], [7]. The stand is based on the construction of ballistic pendulum with the following measuring characteristics: the impact velocity  $V_p$ , residual velocity  $V_r$  and the impact force  $F(t)$  of the target against the dynamometer.

The constructional shields include double layers 6 mm thick of AlZn5Mg2CrZr alloy that has 378 MPa yield strength as well as shields made of ship steel of 230 MPa yield strength. Different structures of constructional shields with the air, sand and crushed glass interlayers 0, 6, 12 mm thick are tested under firing 7.62 mm ŁPS bullets with the impact velocity  $V_p$  above  $820 \text{ ms}^{-1}$  [5], [10]. The energy absorbed by the shield is introduced in general form  $V_{BL[R]}^2$  according to Recht's and Ipson's method, and  $V_{BL[Z]}^2$  according to author's method. The ballistic velocities  $V_{BL[R]}$  and  $V_{BL[Z]}$  of double layer steel, steel – aluminium alloy and aluminium alloy shields with air (1, 2), sand (3, 4) and glass (5, 6) interlayers 0, 6, 12 mm thick (S1, S2, S3) are presented in Figs 1a, 2a and 3a. The proper energy  $V_{BL}^2$ , ballistic velocity  $V_{BL}$ , the effectiveness coefficients  $\beta_s$  as well as mass coefficients  $\alpha^2$  and  $\alpha_s^2$  are verified according to tests results [5], [10]. The coefficients  $\alpha_s^2 - A_s^2$  and  $\beta_s - B_s$  of steel, steel – aluminium alloy and aluminium alloy shields with air (1, 2), sand (3, 4) and glass gaps (5, 6) interlayers 0, 6, 12 mm thick (S1, S2, S3) are presented in Figs 4a, 5a and 6a.

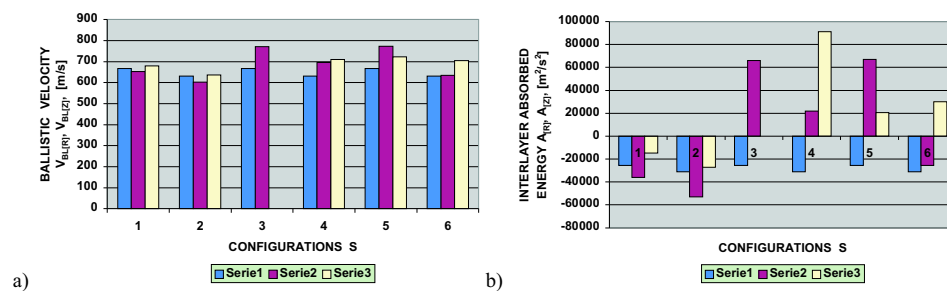


Fig. 1. Ballistic velocities  $V_{BL[R]}$ ,  $V_{BL[Z]}$  – (a) and the effects of interlayer on proper energy absorbed by the shield  $A_{[R]}$ ,  $A_{[Z]} = A_{a1,b1}^6$  – (b) of double-layer steel shields (S) with air (1, 2), sand (3, 4), and glass (5, 6) interlayers 0, 6, 12 mm thick (S1, S2, S3)

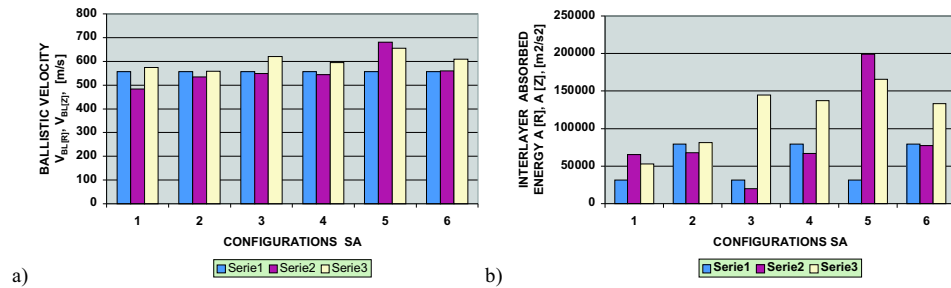


Fig. 2. Ballistic velocities  $V_{BL[R]}, V_{BL[Z]}$  – (a) and the effects of interlayer on proper energy absorbed by the shield  $A_{[R]}, A_{[Z]} = A_{a1,b1}^6$  – (b) of steel – aluminium alloy shields (SA) with air (1, 2), sand (3, 4), and glass (5, 6) interlayers 0, 6, 12 mm thick (S1, S2, S3)

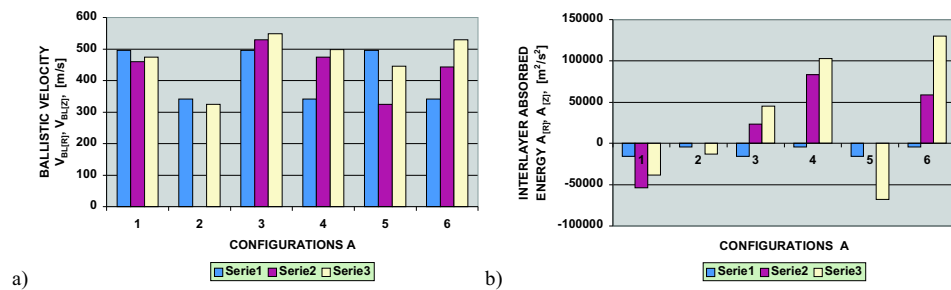


Fig. 3. Ballistic velocities  $V_{BL[R]}, V_{BL[Z]}$  – (a) and the effects of interlayer on proper energy absorbed by the shield  $A_{[R]}, A_{[Z]} = A_{a1,b1}^6$  – (b) of double-layer aluminium alloy shields (A) with air (1, 2), sand (3, 4), and glass (5, 6) interlayers 0, 6, 12 mm thick (S1, S2, S3)

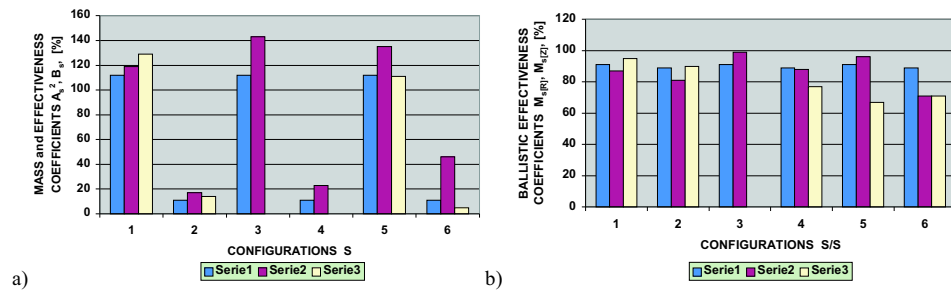


Fig. 4. Mass coefficients  $\alpha_s^2 - A_s^2$  and effectiveness coefficients  $\beta_s - B_s$  – (a) and relative mass effectivenesses  $M_{s[R]}, M_{s[Z]}$  – (b) of double-layer steel shields (S) with air (1, 2), sand (3, 4), and glass (5, 6) interlayers 0, 6, 12 mm thick (S1, S2, S3) against steel plate (S/S)

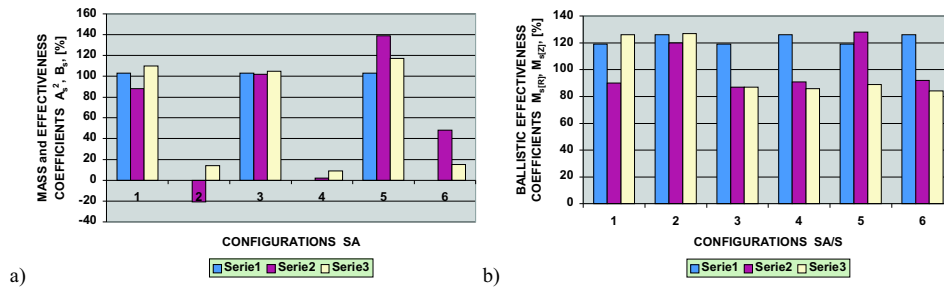


Fig. 5. Mass coefficients  $\alpha_s^2 - A_s^2$  and effectiveness coefficients  $\beta_s - B_s$  – (a) and relative mass effectivenesses  $M_{s[R]}, M_{s[Z]}$  – (b) of steel – aluminium alloy shields (SA) with air (1, 2), sand (3, 4), and glass (5, 6) interlayers 0, 6, 12 mm thick (S1, S2, S3) against steel plate (SA/S)

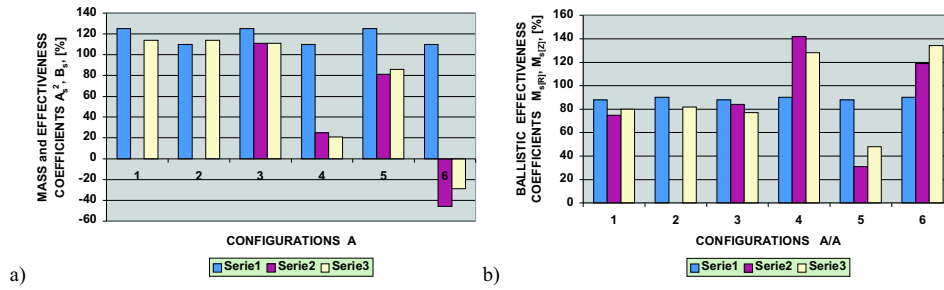


Fig. 6. Mass coefficients  $\alpha_s^2 - A_s^2$  and effectiveness coefficients  $\beta_s - B_s$  – (a) and relative mass effectivenesses  $M_{s[R]}, M_{s[Z]}$  – (b) of double-layer aluminium alloy shields (A) with air (1, 2), sand (3, 4), and glass (5, 6) interlayers 0, 6, 12 mm thick (S1, S2, S3) against aluminium alloy plate (A/A)

#### 4.2. Evaluation of relative mass effectiveness of constructional shields

The mass effectiveness  $M$  of different light armours against 7.62 mm AP bullets is best characterized by comparing their areal density, which is their mass per unit area, with that of RHA

$$M = \frac{(\rho \cdot h_{BL})_{RHA}}{(\rho \cdot h_{BL})_x} \quad (22)$$

where:

$(\rho \cdot h_{BL})_{RHA}$  – the areal density of rolled homogenous steel armour (RHA);  
 $(\rho \cdot h_{BL})_x$  – the areal density of the  $x$  material plate,  $h_{BL}$  thick [12].

The mass effectiveness  $M$  differs from  $M_h$  which is derived from hydrodynamic theory [13]. It results from the limitation of the impact velocity, and from the influences of tensile strength and hardness of the materials. On the other hand, the relative mass effectiveness  $M_s$  of multi – layered shields can be characterized by comparing their areal density with that of

homogenous plate at the same areal energy  $(\rho \cdot h_{BL})_x \cdot V_{BL}^2$  providing the same degree of protection against a given threat

$$M_s = \frac{(\rho \cdot h_{BL})_x}{(\rho \cdot h_{BL})_s} = \frac{V_{BLs}^2}{V_{BLx}^2} \quad (23)$$

where:

$V_{BLx}^2, V_{BLs}^2$  – proper energy absorbed by homogenous plate and constructional shield,

$(\rho \cdot h_{BL})_s$  – areal density of multi – layered constructional shield

$$(\rho \cdot h_{BL})_s = \sum_{i=1}^k \rho_i \cdot h_i \quad (24)$$

where:  $\rho_i, h_i$  – the density and the thickness of  $i$ -layer.

The relative mass effectivenesses  $M_{s[R]}$  and  $M_{s[Z]}$  of multi – layered shields are shown in Figs 4b, 5b, 6b and 7. The selection of the shield structure can be made taking into account the effect of interlayers on proper energy absorbed by the shield

$$A_{an,bn}^{Hn} = V_{BL}^2(H_n + b_n) - V_{BL}^2(H_n + b_n - a_n), \quad m^2s^{-2} \quad (25)$$

where:  $A_{an,bn}^{Hn}$  – the effect of  $n$  – interlayer on proper energy absorbed by the shield.

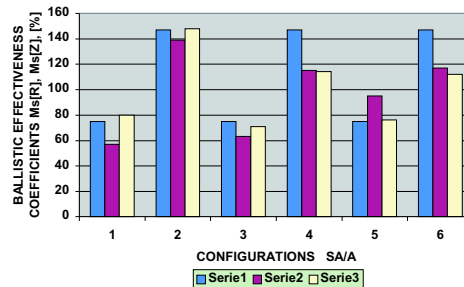


Fig. 7. Relative mass effectivenesses  $M_{s[R]}$ ,  $M_{s[Z]}$  of steel – aluminium alloy shields with air (1, 2), sand (3, 4), and glass (5, 6) interlayers 0, 6, 12 mm thick (S1, S2, S3) against aluminium alloy plate (SA/A)

The values  $A_{[R]}, A_{[Z]} = A_{a1,b1}^6$  are presented in Figs 1b, 2b, 3b for multi – layered shields. The  $n$  – interlayer effectiveness  $N_n$  against proper energy absorbed by homogenous plate takes the following form

$$N_n = \frac{A_{an,bn}^{Hn}}{V_{BLx}^2} = \frac{A_{an,bn}^{Hn}}{V_{BLs}^2} \cdot M_s \quad (26)$$

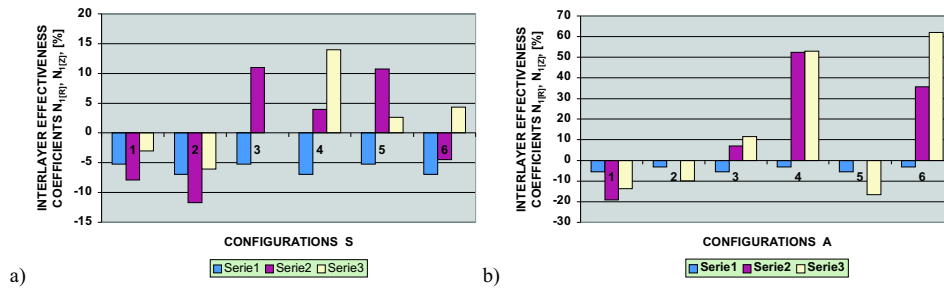


Fig. 8. Interlayer effectivenesses  $N_{1[R]}$  (1, 3, 5),  $N_{1[Z]}$  (2, 4, 6) of double-layer steel shields (S) – (a) and aluminium alloy shields (A) – (b) configurations with air (1, 2), sand (3, 4), and glass (5, 6) interlayers 0, 6, 12 mm thick (S1, S2, S3)

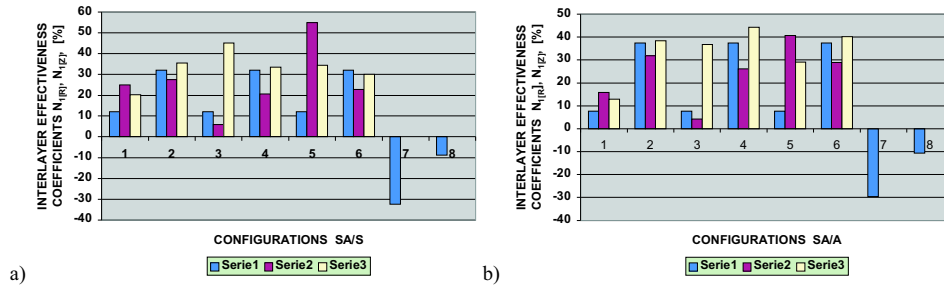


Fig. 9. Interlayer effectivenesses  $N_{1[R]}$  (1, 3, 5, 7),  $N_{1[Z]}$  (2, 4, 6, 8) of double-layer steel – aluminium alloy shields (1, 2, 3, 4, 5, 6), aluminium alloy – steel shields (7, 8) – with air (1, 2, 7, 8), sand (3, 4), and glass (5, 6) interlayers 0, 6, 12 mm thick (S1, S2, S3) against steel plate (SA/S) – (a) and aluminium alloy plate (SA/A) – (b) under firing 7.62 mm ŁPS bullets

The interlayer effectivenesses  $N_{1[R]}$  (1, 3, 5, 7) and  $N_{1[Z]}$  (2, 4, 6, 8) of double layer steel, aluminium alloy and steel – aluminium alloy, and aluminium alloy – steel (7, 8) shields with air (1, 2, 7, 8), sand (3, 4) and glass (5, 6) interlayers 0, 6, 12 mm thick (S1, S2, S3) are presented in Figs 8 and 9. The maximization of interlayer effectiveness  $N_n$  and relative mass effectivenesses  $M_{s[R]}$ ,  $M_{s[Z]}$  facilitates the selection of the shield layers. The effectiveness of methods is determined by effectiveness coefficients  $\beta_s$  and mass coefficients  $\alpha_s^2$ . The above-mentioned coefficients  $\alpha_s^2$  and  $\beta_s$  for steel, steel – aluminium alloy and aluminium alloy shields show high differentiation of ballistic velocities  $V_{BL[R]}$  and  $V_{BL[Z]}$  only for aluminium alloy shields. In this case, ballistic velocity  $V_{BL[Z]}$  must be applied. The relative mass effectivenesses  $M_{s[R]}$  and  $M_{s[Z]}$  attain a maximum for multi – layered steel – aluminium alloy shields with air interlayers 0 and 12mm thick, as well as for the shield with sand interlayer 6 mm thick. The interlayer effectivenesses  $N_{1[R]}$  and  $N_{1[Z]}$  reach a maximum for multi – layer steel – aluminium alloy shields with sand interlayer 12 mm thick or glass interlayer 6 mm thick according to results of firing 7.62 mm ŁPS bullets. Positive values of interlayer effectivenesses

$N_{1[R]}$  and  $N_{1[Z]}$  for double layer steel – aluminium alloy shields, or negative values  $N_{1[R]}$  and  $N_{1[Z]}$  for aluminium alloy – steel shields with air interlayers indicate that the selection of the shield's structure is of primary importance. When the values of all coefficients,  $N_{1[R]}$  and  $N_{1[Z]}$ , as well as  $M_{s[R]}$  and  $M_{s[Z]}$ , approach maxima, one obtains optimum conditions for the selection of multi – layered shields structures.

## 5. Conclusions

1. A new diagnostics method for determining of ballistic resistance of multi-layered shields is described. The proper energy absorbed by the shield is introduced in general form  $V_{BL[R]}^2$  according to Recht's and Ipson's method and  $V_{BL[Z]}^2$  according to author's method.
2. The absorbed kinetic energy of the bullet  $m_p \cdot V_p^2/2$  and the impulse of force  $I$  transferred to the dynamometer of ballistic pendulum are used to determine proper energy  $V_{BL[Z]}^2$  and ballistic thickness  $h_{BL}$  of the shield.
3. The above-mentioned procedure can be widened onto the absorption of the energy by individual layers of the shield, as well as on different grades of metal layers and interlayer areas.
4. The effectiveness of the used methods to determine the proper energy  $V_{BL}^2$  is expressed by effectiveness coefficient  $\beta_s$  as well as by mass coefficient  $\alpha_s^2$ .
5. The maximization of interlayer effectivenesses  $N_{n[R]}$  and  $N_{n[Z]}$  as well as relative mass effectiveness  $M_{s[R]}$  and  $M_{s[Z]}$  leads to optimum conditions for the selection of multi – layered shields structures.

Manuscript received by Editorial Board, February 24, 2006;  
final version, February 16, 2007.

## REFERENCES

- [1] Almohandes A. A., Abdel-Kader M. S., Eleiche Am. M.: Experimental investigation of the ballistic resistance of steel-fibreglass reinforced polyester laminated plates. *Composites*, 1996, Vol. 27B, pp. 447÷458.
- [2] Ben-Dor G., Dubinsky A. and Elperin T.: On the ballistic resistance of multilayered targets with air gaps. *International Journal of Solids and Structures*, 1998, Vol. 35, No. 23, pp. 3097÷3103.
- [3] Bruchey W. J., Burkins M. S.: Suppression of material failure modes in titanium armours. *Proc, 17th Int, Symp. Ballistic, Midrand South Africa*, 1998, Vol. 3, pp. 161÷165.
- [4] Corbett G. G., Reid S. R., Johnson W.: Impact loading of plates and sheets by free – flying projectiles, review. *International Journal of Impact Engineering*, 1996, Vol. 18, No. 2, pp. 141÷230.

- [5] Dobrociński S., Jurczak W., Kolenda J.: Porównawcze badania odporności balistycznej jedno- i dwuwarstwowych próbek ze stopu AlZn5Mg2CrZr i stali kadłubowej kategorii A. Zeszyty Naukowe AMW, 2001, Vol. 146, Nr 2, s. 27÷41.
- [6] Fila J., Zatorski Z.: Podwyższenie odporności balistycznej kadłubów i konstrukcji okrętowych. Raport Nr 1 – 3/1994 – 6/IPBMO/“Powłoka”/AMW-KBN, (unpublished)
- [7] Fila J., Zatorski Z.: Zunifikowane stanowisko do badania odporności balistycznej materiałów, zwłaszcza okrętowych, konstrukcyjno-osłonowych i pancernych. Patent, 1998, AMW, Gdynia.
- [8] Gupta N. K., Madhu V.: An experimental study of normal and oblique impact of hard – core projectile on single and layered plates, International Journal of Impact Engineering, 1997, Vol. 18, No. 5–6, pp. 395÷414.
- [9] Hatrbone H.: Review of recent armor plate developments, Blast furnace and steel plant, 1968, No. 7, pp. 575÷593.
- [10] Jurczak W., Kolenda J.: Badania odporności balistycznej kompozytów ze stopu AlZn5Mg2CrZr i stali kadłubowej z warstwą piasku lub kruszonego szkła. Zeszyty Naukowe AMW, 2001, Vol. 146, Nr 2, s. 51÷66.
- [11] Marom I., Bodner S. R.: Projectile perforation of multi-layered beams. International Journal of Mechanical Sciences. 1979, Vol. 21, pp. 489÷504.
- [12] Mileiko S. T., Sarkissyan O. A., Kondakov S. F.: Ballistic limits of Al-6% Mg alloy plates laminated by diffusion bonding. Theoretical and Applied Fracture Mechanics, 1994, Vol. 21, pp. 9÷16.
- [13] Ogórkiewicz R. M.: Advances in armour materials. International Defense Review, 1991, No. 4, pp. 349÷352.
- [14] Recht R. F., Ipson T. W.: Ballistic perforation dynamics. Journal of Applied Mechanics, 1963, Vol. 30, No. 3, pp. 385÷391.
- [15] Sanguy L., Meunier Y., Pont G.: Steels for ballistic protection. Israel Journal of Technology, 1988, Vol. 24, pp. 319÷326.
- [16] Weimann K., Blache A., Rondot F., et al.: Terminal ballistics of EFPS with high L/D – ratio. 17th Int. Symp. Ballistic, Midrand South Affrica, 23–27 March, 1998, Vol. 3, pp. 161÷165.
- [17] Zatorski Z.: Modelling of energy absorbed under firing of homogeneous plates. Marine Technology Transactions, 2005, Vol. 16, pp. 317÷328.
- [18] Zatorski Z.: Modelling and experimental verifications under firing of energy density absorbed through constructional shields. The Archive of Mechanical Engineering, 2007, Vol. 54, pp. 17÷25.
- [19] Zatorski Z.: Design of ballistic multi – layered steel shields. Marine Technology Transactions, 2006, Vol. 17, pp. 189÷199.
- [20] Recht R. F.: High velocity impact dynamics: analytical modeling of plate penetration dynamics, High velocity impact dynamics, edited by J.A. Zukas, John Willey & Sons Inc. U.K., 1990, pp. 443÷513.

### Diagnostyka odporności balistycznej osłon wielowarstwowych

#### Streszczenie

W prezentowanej pracy opisano metodę diagnostyki odporności balistycznej osłon wielowarstwowych. Wprowadzono energię właściwą absorbowaną przez osłonę w ogólnej postaci  $V_{BL[R]}^2$  zgodnie z metodą Recht i Ipson oraz  $V_{BL[Z]}^2$  zgodnie z metodą autora.

Absorpcja energii kinetycznej pocisku  $m_p \cdot V_p^2/2$  i impuls siły  $I$  przenoszony do dynamometru wahadła balistycznego pozwalają wyznaczyć energię właściwą  $V_{BL[Z]}^2$  i  $V_{BL[R]}^2$  oraz grubość balistyczną osłony  $h_{BL}$ .

Przedstawiona procedura została rozszerzona na absorpcję energii przez poszczególne warstwy osłony oraz różne rodzaje warstw metalowych i obszary międzywarstwowe o odpowiednio dobranych właściwościach balistycznych, gdzie:  $A_{an,bn}^{Hn}$  – efekt  $n$  – tej międzywarstwy na energię właściwą absorbowaną przez osłonę. Efektywność użytej metody do wyznaczenia energii właściwej  $V_{BL}^2$  została wyznaczona przez współczynnik efektywności  $\beta_s$  oraz współczynnik masowy  $\alpha_s^2$ . Maksymalizacja efektywności międzywarstwy  $N_{n[R]}$  i  $N_{n[Z]}$  oraz względnej efektywności masowej  $M_{s[R]}$  i  $M_{s[Z]}$  ułatwia dobór struktury warstw i międzywarstw osłony

Weryfikację metody przeprowadzono na bazie wyników ostrzału osłon wielowarstwowych na opracowanym przez autora i zbudowanym w Akademii Marynarki Wojennej w Gdyni stanowisku do badania odporności balistycznej materiałów.